NASA CONTRACTOR REPORT

NASA CR-61232

June 1968

NASA CR-61232

GPO PRICE $ _____

CSFTI PRICE(S) $ _____

Hard copy (HC) 3,00

Microfiche (MF) .65

ff 653 July 65

CAPABILITY OF THE FPS-16 RADAR/JIMSPHERE SYSTEM FOR DIRECT MEASUREMENT OF VERTICAL AIR MOTIONS

Prepared under Contract No. NAS 8-20082 by
R. E. De Mandel and S. J. Krivo

LOCKHEED MISSILES AND SPACE COMPANY

For

NASA-GEORGE C. MARSHALL SPACE FLIGHT CENTER
Huntsville, Alabama

June 1968

NASA CR-61232

CAPABILITY OF THE FPS-16 RADAR/JIMSPHERE SYSTEM FOR DIRECT MEASUREMENT OF VERTICAL AIR MOTIONS

By

R. E. De Mandel and S. J. Krivo

Prepared under Contract No. NAS 8-20082 by
LOCKHEED MISSILES AND SPACE COMPANY
Huntsville, Alabama

For

Aero-Astrodynamics Laboratory

NASA-GEORGE C. MARSHALL SPACE FLIGHT CENTER

FOREWORD

This document presents the results of work performed by Lockheed's Huntsville Research & Engineering Center while under subcontract to Northrop Nortronics (NSL PO 5-09287) for Marshall Space Flight Center (MSFC) Contract NAS8-20082. This task was conducted in response to the requirement of Appendix A-1, Schedule Order No. 21.

The NASA contract monitor is George Fichtl of the Aerospace Environment Division, Aero-Astrodynamic Laboratory, Marshall Space Flight Center, Alabama.

ACKNOWLEDGMENT

The authors are indebted to Dr. W.A. Bowman of Lockheed/Huntsville's Meteorological Environments Section for his many helpful suggestions during this investigation.

SUMMARY

The FPS-16 radar/Jimsphere system produces highly accurate, detailed measurements of the horizontal component of winds from near the surface to 18 km altitude. Its capability to measure the vertical component, however, whose variations are very small, has not been established. This report evaluates that capability and presents procedures for deriving the vertical wind component from Jimsphere ascent-rate data.

Ascent-rate data contain the effects of vertical air motions as well as measurement errors, balloon response to buoyancy, and other balloon motions not induced by vertical movement of air. The problem of obtaining vertical motions consists of removing the unwanted effects from the data.

Characteristics of measurement error are determined by comparing data obtained from two radars which simultaneously tracked a single Jimsphere. This analysis reveals that random scatter in the 25-m* data is often comparable in amplitude to most variations in vertical velocity which are to be detected. Measurement error, however, contributes primarily to the higher frequencies in the data. Thus it is possible to reduce the threshold of measurement error to a level well below the amplitude of the actual variations in balloon ascent-rate, through application of a suitable low-pass numerical filter.

Empirical and analytical methods are employed to evaluate the balloon's response to buoyant forces. An average ascent-rate profile, computed from 10 Jimsphere flights, reveals that the balloon's upward motion experiences a

*Each 25-m wind value represents an average over a 50-m layer.

gradual, essentially linear decrease with height from the surface up to 15 km altitude. This trend is thought to represent the balloon's response to the normal decrease in atmospheric density with height. Theoretical considerations show that ascent rate is quite insensitive to the density anomalies which might be encountered on any particular flight. It is thus concluded that the effect of buoyancy can be effectively removed from a given ascent-rate profile by subtracting from it an appropriate mean profile.

Other possible sources of vertical balloon motions, including aerodynamically induced oscillations, response to vertical shear in the horizontal wind, and irregular venting of helium from the Jimsphere's release valves, are shown to be unimportant in most cases.

After the above techniques are employed to eliminate the effects of error and buoyancy from ascent-rate measurements, the remaining data measure the vertical component of the wind up to 15 km altitude. It is concluded that these data are best suited for analysis of mesoscale phenomena such as gravity waves and convection. Suggestions are made for further investigations to determine the extent to which the accuracy and resolution of the resultant data might be improved.

CONTENTS

TABLES

ILLUSTRATIONS

Illustrations (Continued)

Section 1
INTRODUCTION

This report covers one phase of a general investigation of the properties of small to mesoscale motions as they relate to space vehicle design, launch and flight criteria. In meteorology, there exists an acute need for a system capable of measuring the vertical component of atmospheric winds. Measurements are needed for the study of such small or mesoscale phenomena as turbulence and gravity waves. Vertical velocities, however, are generally quite small, and therefore difficult to measure in the free atmosphere. Present wind sensing systems are not capable of providing relatively inexpensive detailed measurements of the profile of vertical motion at a given location.

Because the FPS-16 radar/Jimsphere system provides accurate, high-resolution measurements of horizontal wind components up to 18 km, it seems plausible that it could also determine the vertical component. Presumably, the measured ascent rate of the balloon contains the effect of vertical air motions. However, great accuracy is required to measure variations in vertical wind velocity which may be several orders of magnitude smaller than variations in the horizontal components.

The rms error of Jimsphere measurements is less than 0.5 m/sec (Reference 1), where wind values, representing 50-m layer averages, are provided at altitude increments of 25 m. The accuracy and resolution of these measurements represent a major improvement over previous systems such as the rawinsonde. The level of error is very low relative to the magnitude of most horizontal winds. Conversely, it is not small relative to the vertical component, whose actual variations are usually of about the same magnitude.

This may explain why Jimsphere ascent-rate measurements have received little attention.

The crucial problem in this investigation was to find a way to reduce the level of error until it was small compared with the vertical motions that were to be measured. This required a careful examination of the properties of error. The resulting analysis produced some unexpected findings which may lead to improved data acquisition and processing techniques for applications which require very high accuracy.

The overall objectives of this study are: (1) to study the capability of the FPS-16/Jimsphere system to measure vertical air motions; (2) to develop a method to extract vertical motion from available Jimsphere ascent-rate data; (3) to discuss the applications and limitations of the resultant data; and (4) to suggest additional means for improving the quality of the results.

Section 2
DISCUSSION

2.1 CHARACTERISTICS OF JIMSPHERE ASCENT-RATE DATA

The data for this investigation consist of xyz component values of balloon velocity for 25-m intervals of altitude from near the surface to about 18 km. These components were computed from the original 0.1-sec radar position measurements (in spherical coordinates) by a procedure which involves editing, conversion to Cartesian coordinates, smoothing and finite differencing (Reference 2). Editing eliminates position coordinates which appear statistically inconsistent with the surrounding data by replacing each with a local mean. Cartesian position coordinates are then computed. These 0.1-sec data points are then smoothed by averaging over 41 points, and values for each 25 m of altitude are obtained by interpolation. Finally, position coordinates are finite-differenced over 50-m height increments, to produce the three components of balloon velocity. This process appears virtually to eliminate aerodynamically induced balloon motions from the data (Reference 3).

Examination of the three components of motion of a rising Jimsphere (Figures 1 and 3) reveals that variations in ascent rate are comparatively small — about one or two orders of magnitude smaller than those of the horizontal components. Each component can be envisioned as consisting of some mean motion on which a fine structure of high-frequency variations is superimposed.

The ascent-rate profiles shown in Figures 1 and 3 are plotted on an expanded scale in Figures 2 and 4* to illustrate the following characteristics common to ascent-rate data:

1. A significant level of scatter (i.e., high-frequency oscillation) is always observed. Scatter is considered significant if its amplitude approaches the amplitude of the lower frequency oscillations in the data.

2. Large variations in scatter amplitude are observed from one flight to another. Generally, scatter is more pronounced for flights which are made when winds aloft are strong, as in the winter months (Figure 4). Upper winds are not the only criterion, however, since wide variations in the overall level of scatter have been noted between successive flights made during a short period of time when wind conditions aloft were essentially unchanged.

3. Scatter generally becomes more pronounced with increasing altitude. This is apparently because large slant-ranges and low elevation angles are usually associated with tracking a high-altitude balloon.

4. Occasionally, so-called "stray" points (Reference 4) are observed which differ from ordinary scatter in that they are not consistent with the trend nor the high-frequency variations in the data. For example, such stray values are seen in Figure 2 at 4850, 9100 and 14,450 m altitude. In general, stray points are most frequently found at high altitudes.

2.2 INTERPRETATION OF THE DATA

In the first part of this investigation, a method was devised to reduce the threshold of radar error to a level below the amplitude of real variations in ascent rate. Thereafter, the resulting data were assumed to indicate actual motions of the balloon. The next step was to eliminate vertical balloon motions not induced by vertical air motions. Once this was done, the remaining data were considered to represent the vertical component of the wind.

*This scale is used in all subsequent profiles in this report.

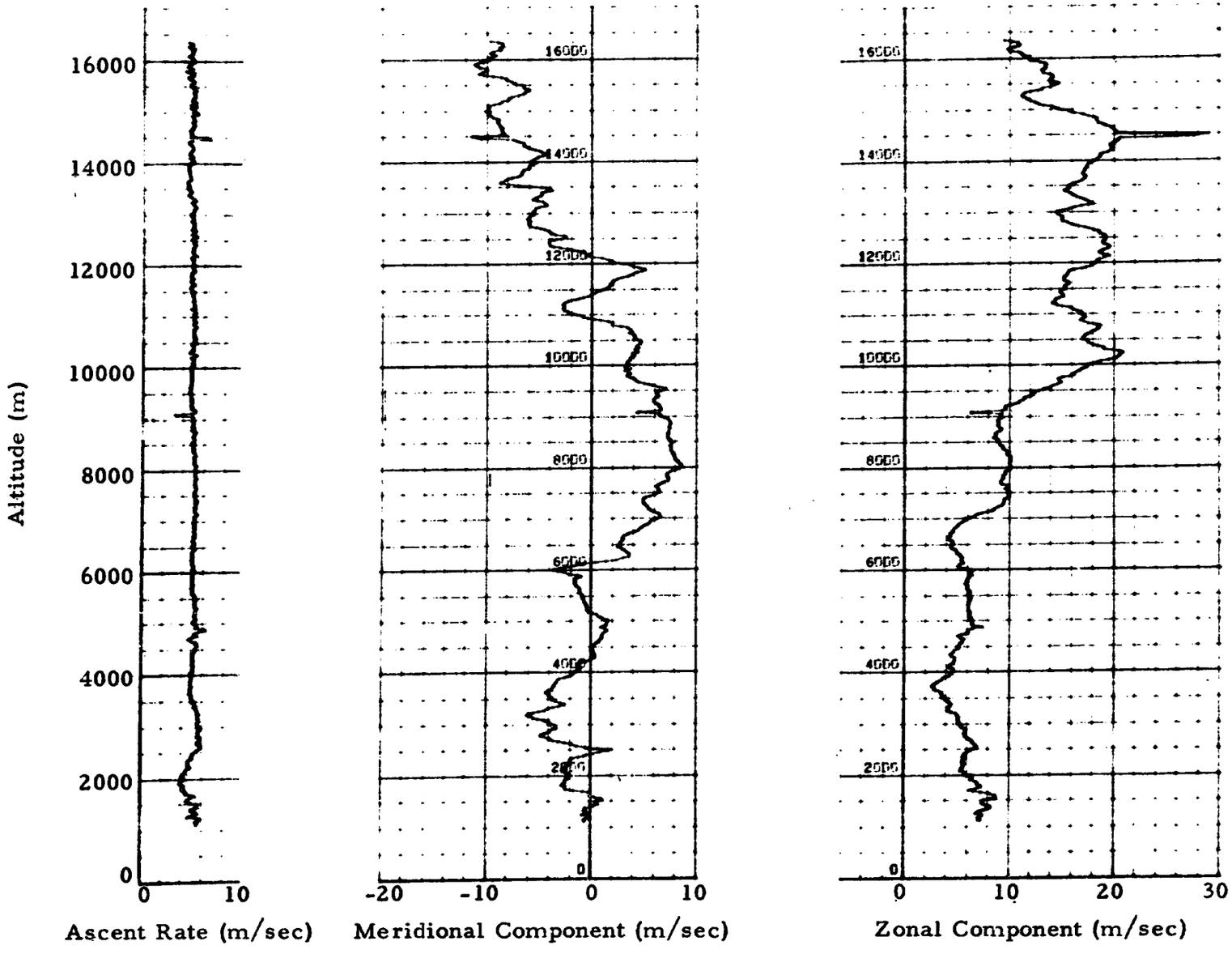

Figure 1 - Components of Jimsphere Motion; 2135Z, 18 April 1967, Cape Kennedy, Florida

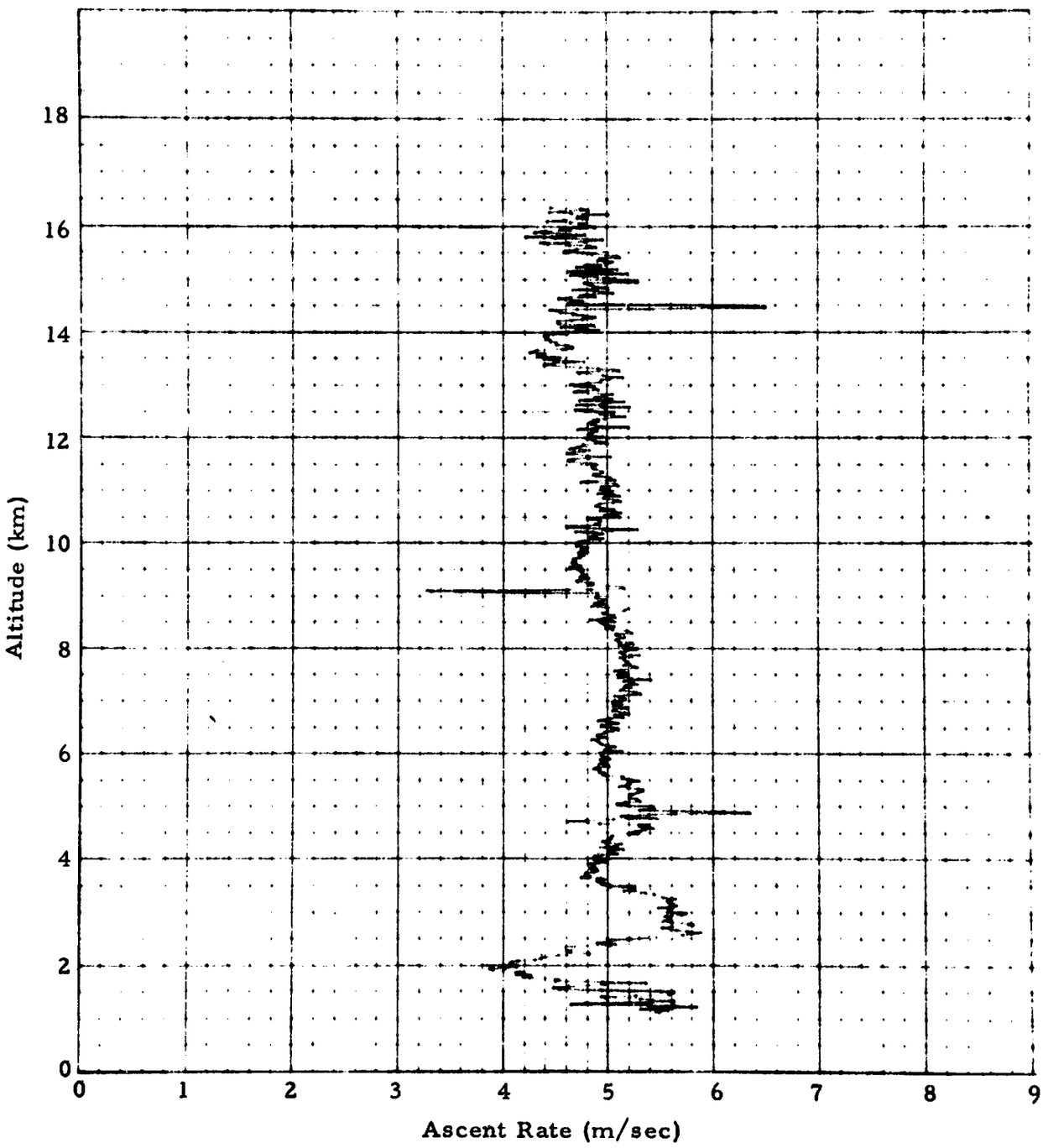

Figure 2 - Ascent-Rate Profile Shown in Figure 1 with Abscissa Expanded Ten Times

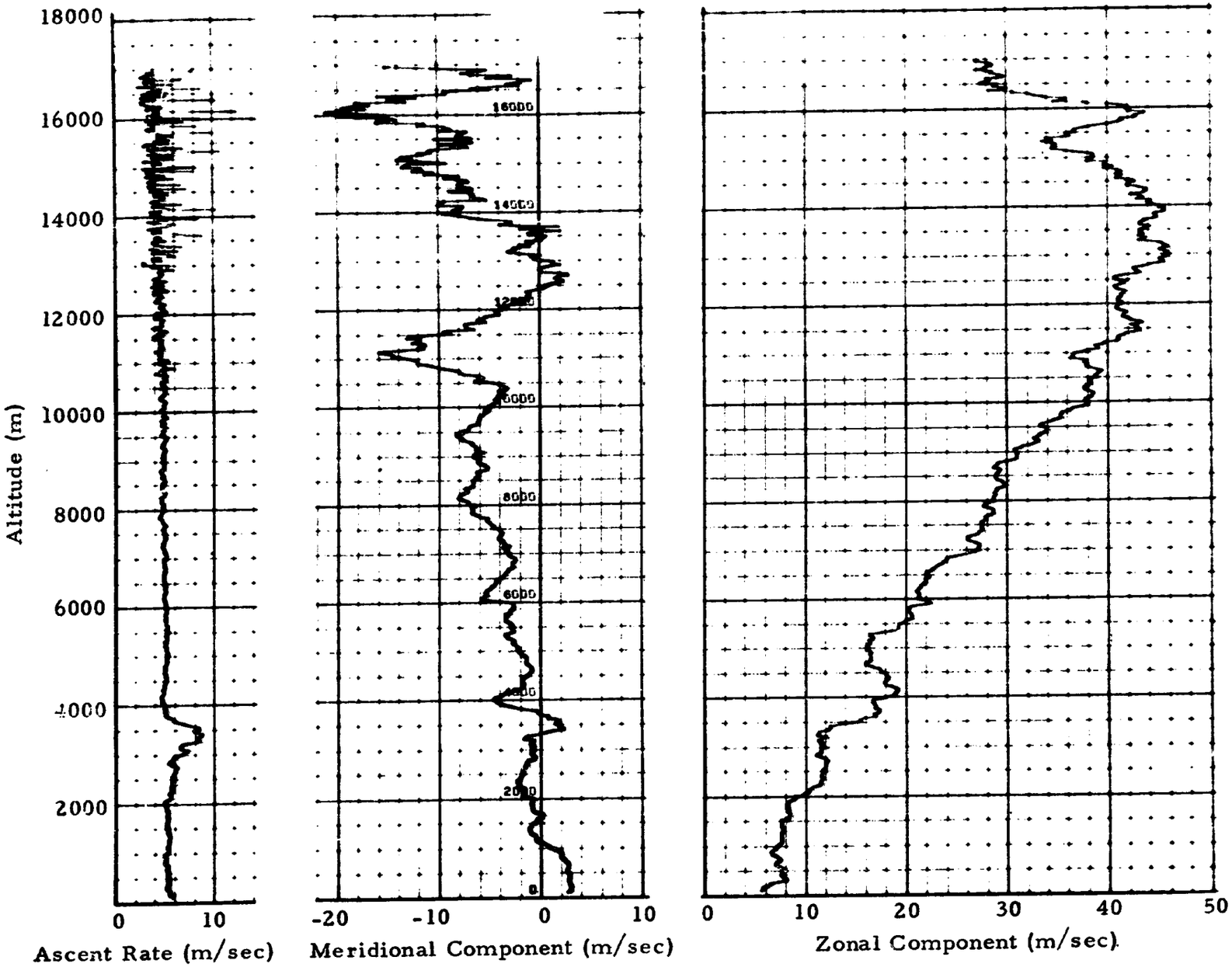

Figure 3 - Components of Jimsphere Motion; 2235Z, 3 February 1967, Cape Kennedy, Florida

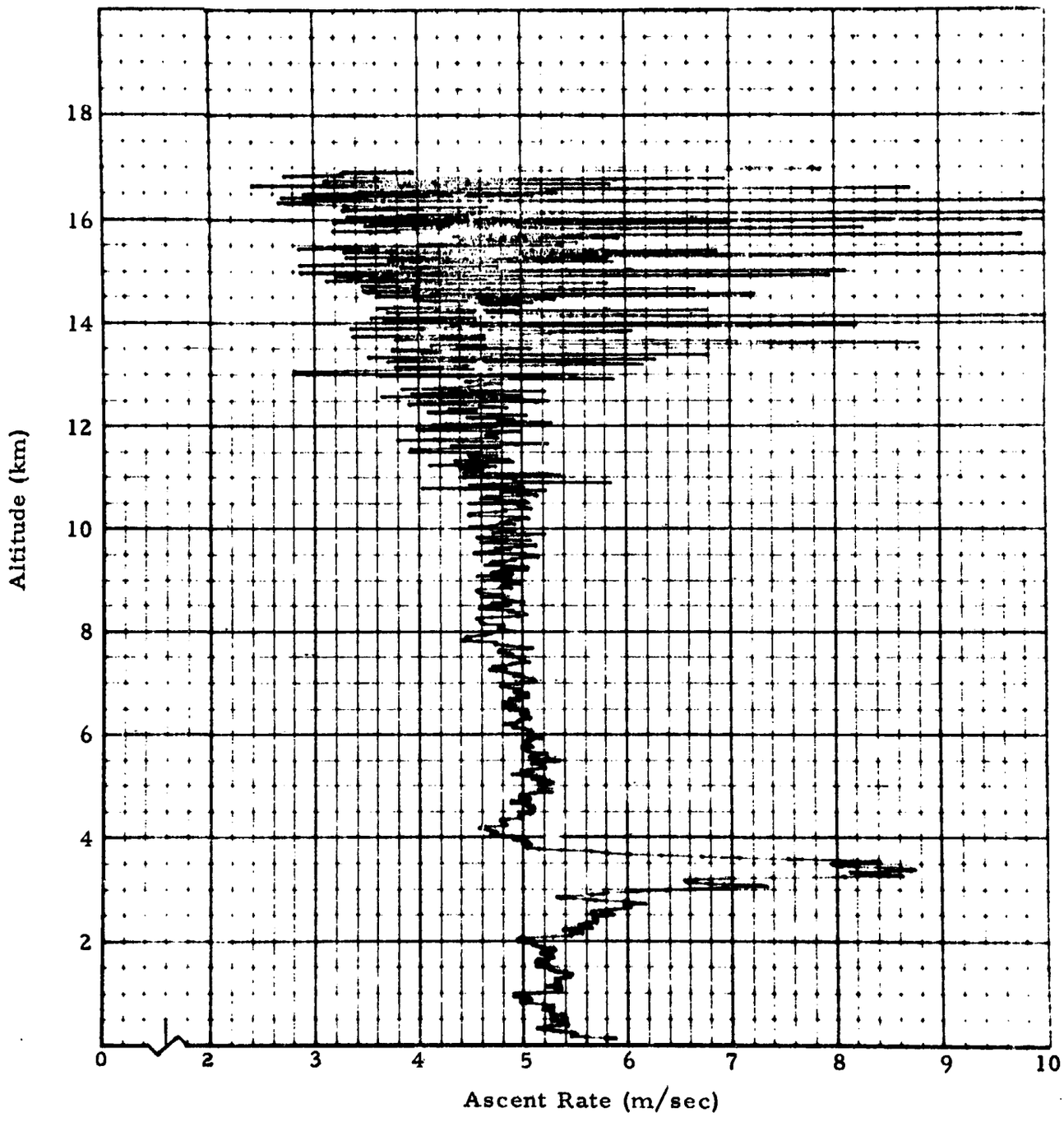

Figure 4 – Ascent-Rate Profile Shown in Figure 3 with Abscissa Expanded Ten Times

2.3 MEASUREMENT ERROR

Tracking error was evaluated by comparing measurements of a single Jimsphere ascent made by two radars operating simultaneously and independently of one another. The resulting ascent-rate profiles are shown in Figure 5. The figure shows that close agreement between the two sets of data is lacking. This is further illustrated in Figure 6, which represents the difference between the two profiles. The rms difference between the two sets of data is about 0.5 m/sec. Clearly, such error is intolerable if vertical motions whose variations are at most a few tens of cm/sec are to be measured.

2.3.1 Random Scatter

Figure 5 reveals that scatter is more intense in Profile A than in Profile B. This difference is at least partially explained by the fact that the two radar sites are about 32 km apart, and the Jimsphere was released close to Radar B. The higher noise level in Profile A reflects the greater slant range (combined with unusually low elevation angles of 1.5° to 10° during the lowest 5 km of the flight) at which Radar A tracked the balloon. Therefore, the level of error suggested by the differences between the two sets of measurements is probably higher than that which exists in most Jimsphere data.

Nevertheless, there is agreement in the lower frequency variations. This indicates that error contributes primarily to the higher frequencies in the data, and might therefore be removed by using a low-pass numerical filter. Determination of an optimum filter for suppressing error was accomplished by applying many different filters and comparing the resultant profiles. The basic filter type used was a 41-point, low-pass, Martin-Graham filter (Reference 5) which has reasonably sharp cutoff characteristics. Only the filter parameters f_c and f_t (the cutoff and termination frequencies define the roll-off interval, $f_c < f < f_t$, and are chosen such that

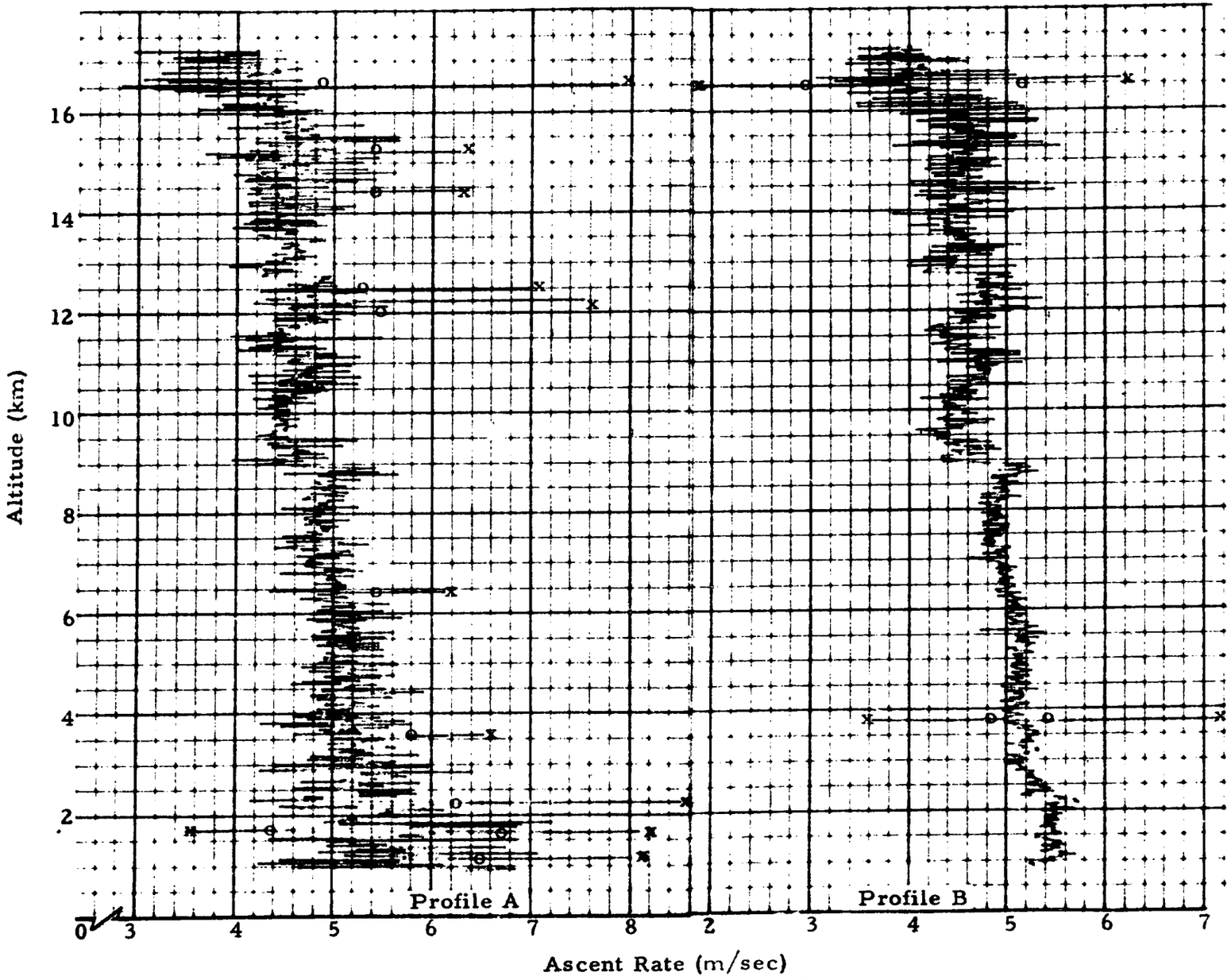

Figure 5 - Simultaneous, Independent Measurements by Two Radars of a Single Jimsphere Ascent; 1400Z, 23 December 1964, Cape Kennedy, Florida

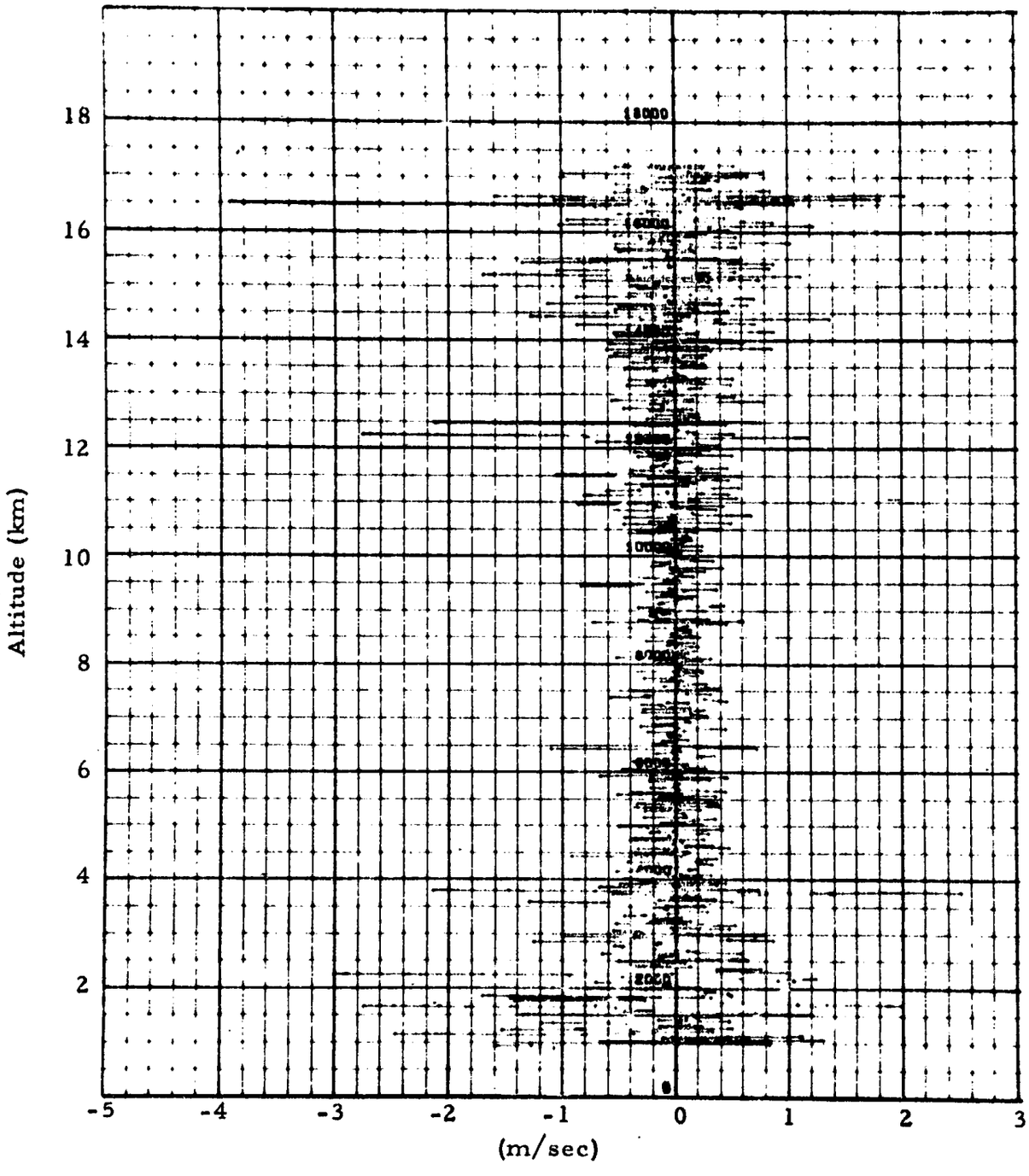

Figure 6 - Residual Profile Obtained by Subtracting Profile A from Profile B

all frequencies lower than f_c are retained, while those greater than f_t are suppressed) were changed from one application to the next. (The theory and application of the Martin-Graham filter are discussed in Appendix A.) Initially, high values of f_c and f_t were used so that only the highest frequencies were suppressed. In the succeeding smoothings, f_c and f_t were progressively decreased, thus suppressing lower and lower frequencies.

The effect of four of the smoothings is illustrated in Figure 7, where in each case the two filtered profiles (A and B) are superimposed. Profile A is represented by unconnected 25-m points, while Profile B appears as a solid line. Values of f_c and f_t, shown for each case, indicate the approximate effect of smoothing. For example, in Figure 7-b all oscillations having frequencies greater than 0.003 cycles/m, i.e., vertical wavelengths ($\lambda = 1/f$) < 333 m, are effectively eliminated. Similarly, any oscillation whose frequency is less than 0.002 cycles/m ($\lambda > 500$ m) is preserved.

Figure 7 shows that smoothing greatly improves the agreement between the two sets of data. This occurs at the cost of reduced resolution. An optimum smoothing process is desired which not only minimizes error but which preserves as much detail as possible. The authors believe that the filter which best satisfies these conditions is the one which produced the profiles shown in Figure 7-b. This judgement is based upon agreement in the 4 to 16 km altitude region only, where scatter in the original data was generally not excessive. The rms differences between Profiles A and B, both filtered and unfiltered, are given for each km of altitude in the second and third columns of Table 1.

An apparent relationship exists between the intensity of scatter in the unfiltered data and the degree of smoothing required to suppress noise. To illustrate, the smoothing which produced the profiles shown in Figure 7-b was apparently sufficient to suppress oscillations resulting from noise

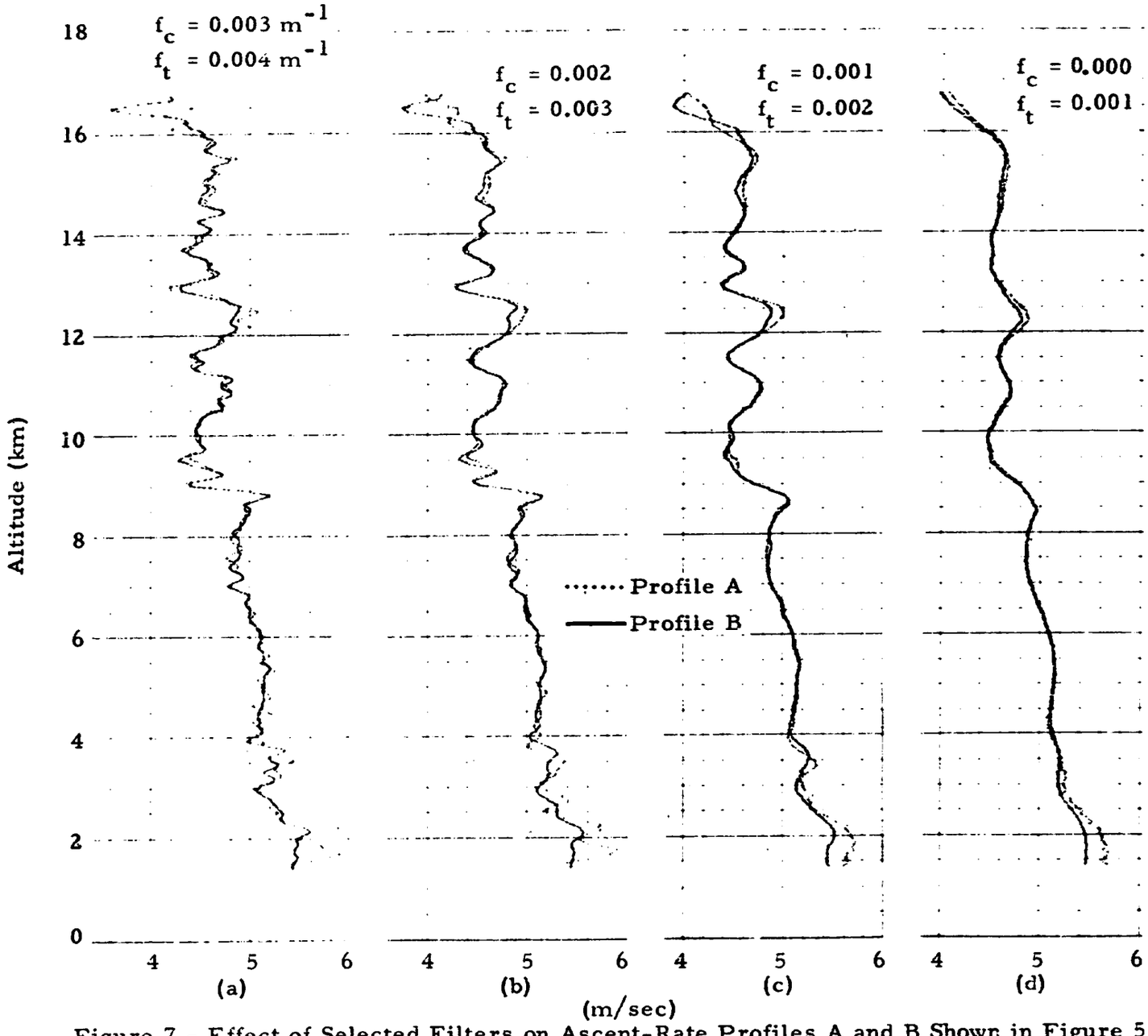

Figure 7 - Effect of Selected Filters on Ascent-Rate Profiles A and B Shown in Figure 5

Table 1

RMS DIFFERENCES BETWEEN PROFILES A AND B

Altitude Interval (m)	(Fig. 6) Non-Filtered Data (m/sec)	(Fig. 7-b) Filtered Data (m/sec)	Edited Filtered Data (m/sec)
2000-2975	0.764	0.150	0.098
3000-3975	0.706	0.117	0.079
4000-4975	0.312	0.045	0.037
5000-5975	0.270	0.017	0.017
6000-6975	0.285	0.015	0.018
7000-7975	0.239	0.034	0.034
8000-8975	0.250	0.033	0.033
9000-9975	0.242	0.069	0.069
10000-10975	0.302	0.018	0.018
11000-11975	0.378	0.025	0.025
12000-12975	0.677	0.082	0.066
13000-13975	0.345	0.027	0.028
14000-14975	0.534	0.042	0.086
15000-15975	0.616	0.051	0.066
16000-16975	0.984	0.065	0.101

in the 4-16 km region. It did not, however, eliminate the effect of intense scatter in Profile A, below 4 km. This observation is important. It implies that for data with a low noise level, error can be suppressed without sacrificing as much detail as when the noise level is high. In the case of Profile A, which has high scatter, it was shown that it is possible to retain only those oscillations having wavelengths of 500 m or more in order to achieve adequate noise suppression. For ascent-rate profiles having low scatter, as in the case of Profile B, it may be possible to preserve shorter wavelengths, perhaps as short as 150 or 250 m.

If the relationship between scatter amplitude and the degree of smoothing required to suppress noise could be defined quantitatively, it would be possible to prescribe an optimum smoothing for any given ascent-rate profile. The use of several sets of dual Jimsphere measurements is suggested to perform an objective analysis, using the technique of successive smoothing described above, to define such a relationship. Then it would be possible to determine optimum values of f_c and f_t as functions of the scatter in any given ascent-rate profile.

2.3.2 Editing and "Stray" Points

It seems reasonable to assume that if data which are inconsistent with surrounding values were removed from the 25-m data prior to smoothing, accuracy could be improved. Such stray points appear in both of the profiles in Figure 5. Since they do not occur at corresponding altitudes, they must be erroneous. To test the effect of editing, the points indicated by x's in Figure 5 were replaced with values which were more consistent with surrounding data, indicated by o's. The last column in Table 1 gives the rms differences between the two edited, filtered profiles. It is seen that at some levels (2 to 5 km and 12 to 13 km) agreement was improved, while at others (6 to 7 and 13 to 17 km) agreement was poorer. Overall, the editing produced no significant improvement in agreement between the two profiles.

The above result shows that data editing, without prior knowledge of the cause of the error, can be poor practice. For example, if stray points are known to result from random voltage fluctuations in the circuitry of the radar which are wholly independent of the motions of the target, it is reasonable to assume that editing will improve the quality of the data. If, on the other hand, stray points result from occasional abrupt adjustments of the tracking antenna, rejection of these points can reduce the accuracy of the data, as will now be shown. Consider two simplified hypothetical cases where a balloon is due east of the radar and moving eastward at constant velocity (Figure 8). On the left of the figure actual balloon positions are represented by circles and measured positions are indicated with crosses. Velocity is computed by taking backward differences between adjacent position measurements. In Case I, the radar momentarily "loses" the target between the fourth and sixth points and thus records an inaccurate measurement at the fifth point. The resulting velocity profile on the right side of the figure contains two stray points. Because these points are equidistant from the mean, or actual, velocity, editing (i.e., replacing them with the local mean value derived from surrounding points) of both points preserves the mean of the whole set of points. Here, editing has the same effect as smoothing. In Case II, however, where the radar allows the target to drift slowly off center and then abruptly corrects, only one stray point is produced in the resulting velocity profile. If this point is replaced by the local mean value, the mean of the whole sequence of points is erroneously increased from 1.0 to 1.5.

The basic Jimsphere data processing routine which computes 50-m layer values of wind velocity from the 0.1-sec range, azimuth and elevation angle measurements of the radar, contains an editing procedure which statistically rejects stray points. Unless all such points are known to be completely independent of the movement of the tracking antenna, it is suggested that their rejection may in some cases reduce data accuracy.

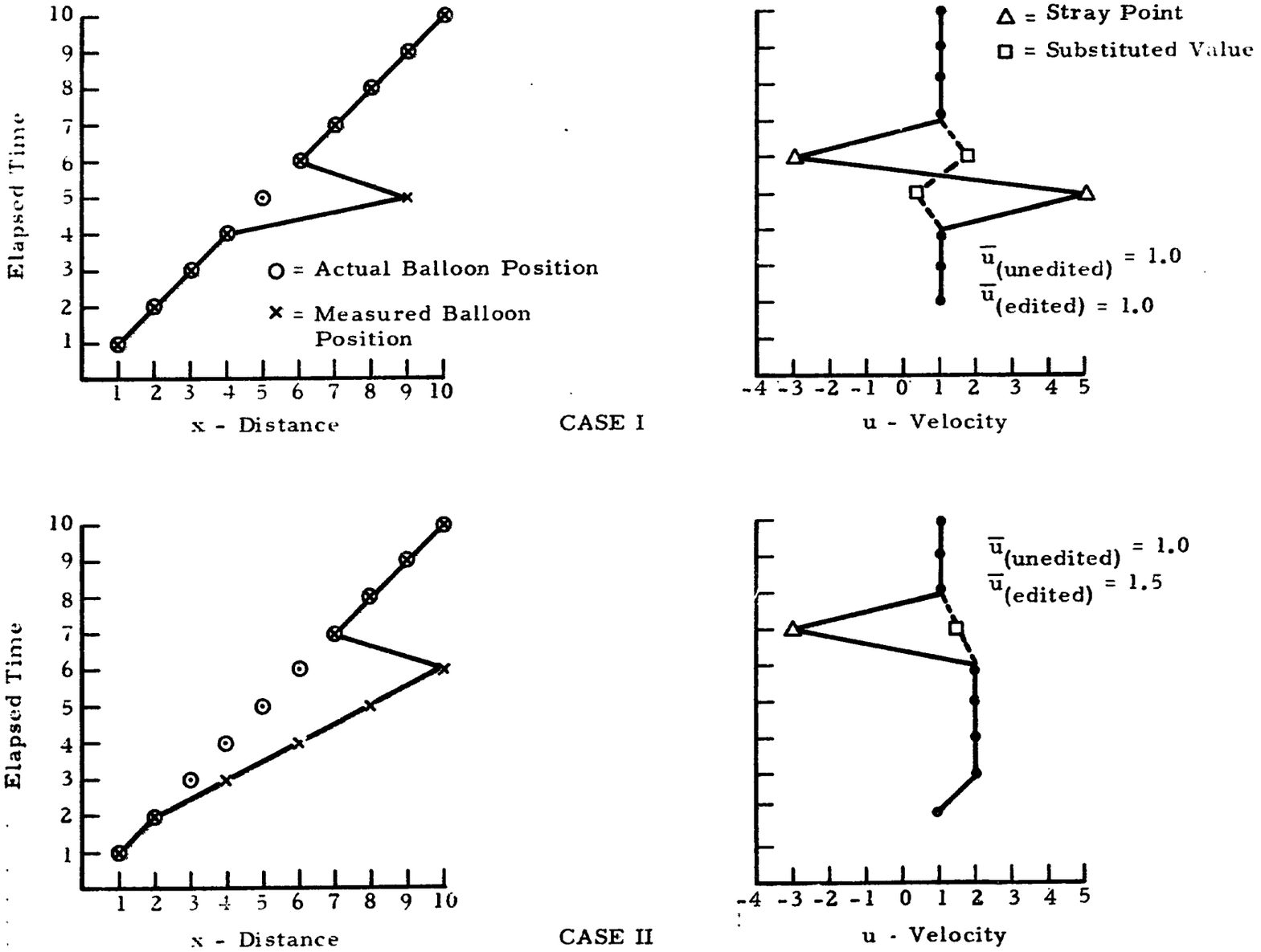

Figure 8 - Two hypothetical cases illustrating possible effects of editing "stray" data points. Units are arbitrary. Editing consists of replacing stray points with an average based on the three values preceding and following that point.

2.3.3 Biasing

Analysis of ascent-rate measurements indicates that systematic errors sometimes occur in the processed data. For example, inspection of 30 filtered ascent-rate profiles reveals that when scatter becomes excessive, as in Figure 4 above 13 km, the mean (or smoothed) ascent rate becomes unusually high. This effect is also evident in Figure 7-d where, at levels where scatter in Profile A was high, the smoothed values of Profile A exceed those of Profile B. In the next section it will be shown that the mean ascent rate of the Jimsphere, when smoothed over relatively large altitude intervals (of the order of 1 to 2 km), is reasonably constant from one sounding to the next. When intense scatter is present, however, ascent-rate measurements may be biased toward values as much as 1.5 m/sec higher than expected. Therefore, no attempt was made in this investigation to compute vertical motions in regions of excessive scatter.

It may be that biasing of ascent-rate values is associated with the occurrence of stray points in the 25-m data. There appears to be a positive correlation between scatter intensity and the incidence of stray points. Further, it is noted that stray points are usually high-valued. That is, few low-valued stray points are encountered, as Figure 4 shows. It is not yet known whether biasing is caused by systematic errors in radar measurements or whether it is produced by data processing.

2.3.4 Summary

In this section it was shown that random and systematic errors in Jimsphere ascent-rate data may be comparable in magnitude to the small vertical wind variations we wish to measure. Therefore, treatment of error is a crucial step in the derivation of vertical motions. Errors in the horizontal components are known to be of approximately the same magnitude (i.e., generally 0.5 m/sec or less). This level of error is negligible in comparison with measured variations in horizontal components, and this is not

significant in most space vehicle engineering and meteorological applications of Jimsphere wind data. Error in the horizontal components would be important, however, in investigations of the high-frequency spectral content of the winds.

The smoothing technique employed here reduced the level of error by nearly an order of magnitude, thus making reasonably accurate ascent-rate data possible. This increase in accuracy, however, was achieved by sacrificing resolution to the point where all wavelengths shorter than 333 m were lost. The authors believe that, with further research, resolution can be improved considerably. This can be done by: (1) analyzing dual data which are more representative of most Jimsphere measurements (i.e., data containing less scatter than those used here); and (2) seeking improved methods for processing (editing and smoothing) the 0.1-sec radar data. Specific recommendations for future investigations are made later in this report.

2.4 THE CONTRIBUTION OF BUOYANCY TO THE MOTION OF A JIMSPHERE

The digital filtering employed in the preceding discussion reduced Jimsphere ascent-rate measurement error to an rms level of about 5 cm/sec. Within the limitations imposed by this error, it is assumed that variations in smoothed data represent actual balloon motions. The remaining task is to eliminate any balloon motion not induced by vertical air motions. The most important of these is the response of the Jimsphere to buoyancy.

An ascending balloon experiences continually varying buoyant and drag forces. Thus, its ascent rate continually changes. It is useful to make a distinction between the systematic decrease in ascent rate associated with the normal decrease in atmospheric density with altitude, and nonsystematic variations resulting from density anomalies encountered during a particular flight. The systematic effect is shown to be easily removed from the data. Nonsystematic variations are shown to be small, at least up to 15 km altitude.

2.4.1 Systematic Buoyancy Variations

The systematic effect could be estimated from a mean ascent-rate profile, computed from a large sample of observations. Presumably, variations in individual profiles due to vertical air motions or other non-systematic effects would tend to cancel in the averaging process. The mean profile could then be subtracted from an individual ascent-rate profile, yielding a measurement of variations in the ascent rate of the balloon. These variations would include the effects of vertical air motions.

To illustrate this procedure, a mean profile was used based on 10 Jimsphere flights made during December 1964 (Reference 6). Mean ascent-rate values are listed at 1-km altitude intervals in Table 2. From the surface to 15 km the profile is almost linear. Thus, to simplify computation, a least-squares linear fit to the first 15 1-km values is taken to represent the systematic response of the Jimsphere to buoyancy. The procedure used to derive a profile of nonsystematic variations in ascent rate is illustrated in Figure 9. (It is shown below that the resultant data are essentially a measure of vertical air motions.) The 41-point filter discussed in Appendix A (see Figure A-1) is used to smooth the original ascent-rate data. The systematic effect of buoyancy is then removed by subtracting the linearized mean ascent rate.

The method shown involves computing a mean profile for December and applying this profile to a single observation made during that month. Similar mean profiles could be constructed for the other months, using as many observations as possible for the computation of each mean profile. This method contains the implicit assumption that day-to-day variations in atmospheric density within a given month do not significantly affect the Jimsphere's ascent rate. The following discussion shows that this is a reasonable assumption up to 15 km altitude.

Table 2

AVERAGE VALUES OF ρ, T, p AND w FOR DECEMBER AT CAPE KENNEDY, FLORIDA

Altitude (km)	Average Measured Ascent Rate (cm/sec)	IRIG Range Reference Atmosphere December, Cape Kennedy ρ(g/cm^3) x 10^{-6}	T(^{o}K)	p(dynes/cm^2) x 10^{-3}	C_D (computed)
0	—	1209.7	291.7	1019.8	—
1	530	1098.2	286.3	907.2	0.722
2	523	989.5	282.5	805.0	0.732
3	520	891.5	278.3	713.0	0.730
4	508	804.5	272.8	630.0	0.752
5	500	725.1	266.8	555.4	0.762
6	500	653.4	260.2	488.1	0.746
7	497	588.5	253.0	427.4	0.738
8	487	528.5	245.8	372.9	0.748
9	478	473.6	238.3	324.0	0.752
10	470	422.9	230.8	280.2	0.748
11	466	376.6	223.1	241.2	0.726
12	460	332.8	216.4	206.7	0.702
13	460	290.2	211.5	176.2	0.646
14	460	250.4	208.7	150.0	0.580
15	456	215.3	206.0	127.3	0.510
16	438	185.0	203.1	107.8	0.452
17	383	157.6	201.5	91.1	0.424
18	265	132.8	202.1	77.0	0.450

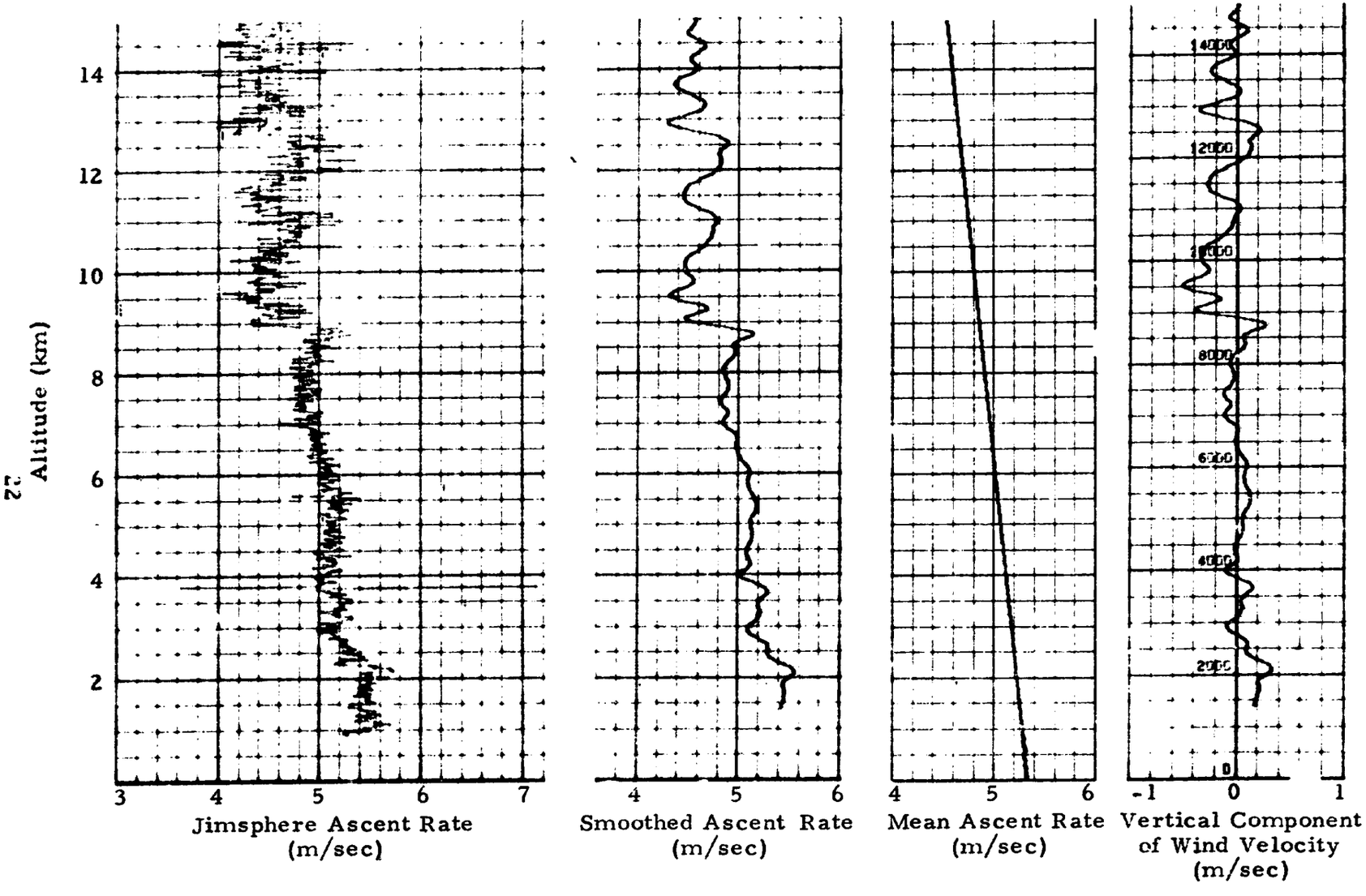

Figure 9 - Procedure Used to Derive the Vertical Wind Component from Jimsphere Ascent-Rate Data

2.4.2 Nonsystematic Buoyancy Variations

Before the observed variations in ascent rate can be attributed to vertical air motions, it must be shown that they are not induced by anomalies in atmospheric density. To do this, the forces acting on the balloon were first analyzed to produce an expression for the ascent rate of the Jimsphere in a motionless atmosphere (Appendix B):

$$C_D w^2 \cong 2.26 \times 10^5 - 25.5 \rho^{-1} \qquad (1)$$

where C_D is the drag coefficient, w is the balloon's ascent rate, and ρ is atmospheric density.

Thus, w is a function of C_D and ρ. The drag coefficient varies throughout a Jimsphere ascent (Reference 6). Values of C_D are shown in Table 2 at 1-km increments of altitude. These were computed from Equation (1) using the mean values of w described above and values of ρ provided by IRIG Range Reference Atmosphere data for December at Cape Kennedy (Reference 7). Below 12 km C_D is reasonably constant, while above 12 km, it decreases markedly.

The perturbation method is used to derive an expression for the effect upon w of a perturbation in ρ. We assume that the three variables may be represented as sums of mean and perturbation quantities.

$$w = \overline{w} + w'$$

$$C_D = \overline{C}_D + C_D'$$

$$\rho = \overline{\rho} + \rho'$$

where bars indicate mean quantities and primes indicate perturbation quantities. We also assume that both the total quantities and the mean quantities satisfy Equation (1). If the equation for the mean motion is subtracted from the equation for the total motion and the resulting expression is solved for w', we obtain:

$$w' = -\bar{w} + \left(\frac{\bar{C}_D}{\bar{C}_D + C_D'}\right)^{1/2} \cdot \left(\bar{w}^2 + \frac{25.5}{\bar{C}_D} \frac{\rho'}{\bar{\rho}\,(\bar{\rho}+\rho')}\right)^{1/2} \qquad (2)$$

Equation (2) can be used to determine how w is affected when the Jimsphere encounters an anomalous variation in density. Consider, for example, a hypothetical case where the balloon passes through a density discontinuity at 9 km altitude, where density above the boundary is 4% less than it is below. Meteorologically, this is a rather extreme case – equivalent to a 10°C temperature jump at 9 km. Equation (2) is solved by taking values of $\bar{\rho}$, $\bar{C}_D$ and $\bar{w}$ from Table 2. The quantity ρ' is taken to be $-0.04\bar{\rho}$. Further, since C_D is essentially constant up to 12 km, C_D' is assumed to be zero. When the above substitutions are made, we obtain

$$w' \cong -4 \text{ cm/sec}$$

Thus, passage of the balloon through a sharp density discontinuity produces a change in ascent rate of only a few cm/sec. The same calculation was made for each of the 1-km altitude increments. Only above 15 km, where the balloon approaches its floating level, did w' exceed a few cm/sec. For this reason, and because C_D' is difficult to evaluate at higher altitudes, vertical motions are computed only up to 15 km in this study.

It is concluded that the ascent rate of the Jimsphere is relatively insensitive to anomalous variations in atmospheric density. Therefore, major nonsystematic variations in ascent rate may not be attributed to thermodynamic effects. This insensitivity of the Jimsphere to anomalies in atmospheric density also supports the assumption that a mean profile may be used to approximate the balloon's response to buoyancy on a given day.

Because the thermodynamic effects do affect the motion of the Jimsphere, even though only slightly, derivation of vertical motions could be made more accurate, were these effects taken into account. If w' could be computed as a function of altitude for a given flight, it could be removed, along with the systematic effect, from the measured data. To do this effectively, it would be necessary to define the relationship between w, C_D and ρ more accurately, and to obtain simultaneous high-resolution temperature data with each Jimsphere flight. Such data may soon be available following the development of a fast-response temperature sensor to be flown with the Jimsphere.

2.5 OTHER FACTORS INFLUENCING BALLOON MOTION

In the preceding discussion, a measure of vertical balloon motion was derived from which the effects of buoyancy and measurement error had been essentially removed. Before it is concluded that the data reflect vertical air motions, however, other sources of balloon motion must be considered. These include: (1) aerodynamically induced balloon motions; (2) condensation of moisture or accumulation of ice on the balloon; (3) irregular venting of helium from the release valves; and (4) response of the balloon to vertical shear of the horizontal wind.

2.5.1 Aerodynamically Induced Balloon Motions

The Jimsphere is known to experience aerodynamically induced oscillations having a period of about 4.5 sec (Reference 3). Even if these motions are not completely removed when the 0.1-sec radar data are smoothed to produce the 25-m values, they are certainly suppressed by the additional filtering used to reduce the effect of measurement error.

2.5.2 Icing and Condensation

As a balloon ascends through cloud layers, moisture or ice may collect on its surface, thereby increasing its weight and reducing lift. Since the effects of icing and condensation are difficult to evaluate, it is suggested that until more is known about this problem, vertical motions be computed only for those cases when these phenomena were not likely to have occurred.

2.5.3 Irregular Venting of Helium

If the valves which vent helium in order to maintain the internal superpressure of the Jimsphere at a constant 5 mb were to release the gas in occasional spurts, rather than continuously, spurious variations in lift would result. To determine if this effect could produce significant variations in ascent rate, we refer to Appendix B, Equation (B.11). The superpressure s appears only in the C_3 term. Since (C_3/T_b) was shown to be small enough that it could be neglected in Equation (B.13), it follows that variations in s of a few mb would have little effect upon w.

2.5.4 Response of the Balloon to the Vertical Shear of the Horizontal Wind

In the analysis of the forces acting on a rising Jimsphere (Appendix B), a motionless atmosphere was assumed. Actually the balloon ascends through shear layers, and because of inertia, it does not instantaneously respond to

the changing wind field. Thus, the relative wind (i.e., the resultant wind experienced by the balloon — can be envisioned as the wind which would be measured by a sensor attached to the balloon) may differ somewhat from -w, which is the relative wind in the absence of shear. This produces a corresponding change in the drag force.

To determine if the change in relative wind associated with wind shear has a significant effect upon the rate at which the Jimsphere rises, consider a balloon ascending through an atmosphere in which the horizontal wind varies with altitude. For simplicity, the vertical wind component is assumed to be zero. The buoyant and gravitational forces are the same as in the previous analysis (Appendix B). The vertical component of the drag force is given by

$$D_z = -1/2\, C_D\, \rho\, A\, V_R\, w$$

where V_R is the velocity of the relative wind (Reference 8). It is easily shown that

$$V_R = \sqrt{(v - \dot{x})^2 + w^2}$$

where v is the horizontal wind velocity, and $\dot{x}$ is the horizontal velocity of the balloon.

Using $\hat{D}_z$ to denote the drag force which is computed when the effect of shear is taken into account and D_z to denote the drag force computed when shear is neglected, we obtain the ratio of these quantities:

$$\hat{D}_z/D_z = \frac{\sqrt{(v - \dot{x})^2 + w^2}}{w} = \sqrt{\frac{(v - \dot{x})^2}{w^2} + 1}$$

Eckstrom and others (Reference 6), have shown that for practical purposes $(v - \dot{x}) \leq 50$ cm/sec. Further, during a Jimsphere flight (surface to 15 km), w generally exceeds 450 cm/sec. Therefore,

$$1 \leq \frac{\hat{D}_z}{D_z} \leq \sqrt{\frac{50^2}{450^2} + 1} = 1.006$$

or

$$D_z \leq \hat{D}_z \leq 1.006\, D_z \quad .$$

If $1.006\, D_z$ is substituted into Equation (B.5) in Appendix B, it is found that w is changed by no more than 1.5 cm/sec. Furthermore, because the extreme wind shears which could produce this change occur over very thin layers, this effect would extend over a small vertical distance. Consequently, it would undoubtedly be removed by filtering. It is concluded that wind shear has a negligible effect upon the vertical component of motion of the Jimsphere.

Section 3
CONCLUSIONS

It has been shown that a measure of the vertical wind component may be derived from Jimsphere ascent-rate data. This is possible despite the high noise level in the original data and despite the difficulty in distinguishing between balloon response to buoyancy and response to vertical air motions. The data processing procedures set forth in this document may be implemented to derive vertical motions from any existing FPS-16/Jimsphere data.

The investigation of measurement error showed that error is confined primarily to the higher frequencies and therefore can be greatly reduced by applying a suitable low-pass filter. It was shown that when the noise level is low, less smoothing is necessary, thus allowing for more detail in the smoothed data. It was demonstrated that editing of stray points, without prior knowledge of their cause, can be poor practice. Furthermore, there is strong evidence that the ascent-rate data are biased toward high values in regions where high noise levels are present in the 25-m data. Therefore, a reevaluation of data acquisition and processing procedures may be helpful in establishing techniques for more accurate determination of vertical motions.

Balloon response to anomalies in atmospheric density was found to be very small, at least below 15 km altitude. Thus, the effect of buoyancy on balloon motion can be removed from any given ascent-rate profile by subtracting a mean ascent-rate profile based on many Jimsphere ascents made under similar meteorological conditions.

Balloon motions resulting from aerodynamically induced oscillations, sporadic venting of helium, and passage through shear layers were shown to be negligible. It was recommended that, since the effects of condensation and icing on rate of rise are not presently known, no attempt to derive vertical motions should be made using data acquired when these phenomena were likely to have occurred.

It is estimated that the resultant vertical motion measurements (of vertical wavelengths $\geq$ 333 m) have an accuracy on the order of $\pm$5 cm/sec. Although this is far greater than the accuracy of the original 25-m values, it is not sufficient to analyze the very small vertical motions associated with large-scale events. Furthermore, the extensive filtering which was necessary to reduce noise precludes sufficient resolution to detect most motions of small vertical extent. Thus, the processed data probably best measure mesoscale motions, including such phenomena as gravity waves and local convection. (The large increase in upward motion between 3 and 4 km in Figure 4 is thought to be convective in origin.)

Present data acquisition and processing procedures are quite adequate for the space vehicle engineering applications for which they were originally intended (i.e., for measuring horizontal wind components with an accuracy of perhaps $\pm$0.5 m/sec). If the FPS-16/Jimsphere is to be used for accurate measurement of vertical motions, however, or for obtaining estimates of the high-frequency spectral content of all components, it may be necessary to improve these procedures. It is anticipated that data processing techniques can be improved substantially, thereby providing greater accuracy and resolution than were heretofore available and extending the scale of motions which can be measured by the FPS-16/Jimsphere system.

Section 4
RECOMMENDATIONS

A thorough investigation of the properties and sources of measurement error is needed, including:

- A Careful Review of the Problems Involved in Data Acquisition in the Field: The capabilities and limitations of the FPS-16 radar, its operation and sources of error, should be more precisely defined. For example, it is important to learn the nature and frequency of occurrence of errors associated with electronic malfunction, improper radar operation procedures, atmospheric refraction, excessive ground clutter, attenuation of the signal by clouds or precipitation, tracking at great distances and low elevation angles, and so on. This investigation should include a survey of literature on radar operation and discussions with persons who are intimately familiar with the theory and operation of the FPS-16. The investigation could lead to suggestions for improving operational procedures (such as releasing the balloon upstream to avoid tracking at great distances, etc.).

- An Analysis of the Data Processing Procedures: The effectiveness of present data editing and smoothing schemes should be critically reviewed. This could best be accomplished by comparing measurements of a single Jimsphere by two radars. Several such pairs of measurements should be analyzed so that data processing procedures can be tested

for data obtained under various tracking conditions. These data could be used to evaluate any number of smoothing and editing techniques by noting how these techniques affect agreement between the two sets of measurements. Thus, effective methods for dealing with biasing, intense scatter, and stray points might be found.

The relationship between the balloon's rate of rise and atmospheric density should be more accurately determined. This is because it is necessary to distinguish between balloon response to buoyancy and to vertical air motions. It would be useful to analyze simultaneous, high-resolution wind and temperature measurements for this purpose.

REFERENCES

1. Scoggins, James R., "Sphere Behavior and the Measurement of Wind Profiles," NASA TN D-3994, George C. Marshall Space Flight Center, Huntsville, Ala., June 1967.

2. Biner, Daniel J., "FPS-16 Spherical Balloon Reduction," Document No. 0189, Computer Sciences Corp., Huntsville, Ala., 29 April 1967.

3. Rogers, R.R. and H.G. Camitz, "Project Baldy – An Investigation of Aerodynamically Induced Balloon Motions," NASA Contract NAS8-11140, Marshall Space Flight Center, Huntsville, Ala., 1965.

4. Scoggins, James R., "An Evaluation of Detail Wind Data as Measured by the FPS-16 Radar/Spherical Balloon Technique," NASA TN D-1572, George C. Marshall Space Flight Center, Huntsville, Ala., May 1963.

5. Anders, Edward B., et al., "Digital Filters," NASA CR-136, Prepared under Contract NAS8-5164 by Auburn Research Foundation, Inc., Auburn, Ala., December 1964.

6. Eckstrom, Clinton V., "Theoretical Study and Engineering Development of Jimsphere Wind Sensor," NASA Contract NAS8-11158, The G. T. Schjeldahl Company, Advanced Programs Division, Northfield, Minnesota, July 1965.

7. Atlantic Missile Range Reference Atmosphere for Cape Kennedy, Florida (Part I), Inter-Range Instrumentation Group, IRIG Document 104-63, September 1963.

8. Johnston, Kenneth D., "Response of Spherical Balloon to Wind Gusts," NASA Memorandum M-AERO-A-12-62, George C. Marshall Space Flight Center, Huntsville, Ala., 5 March 1962.

Appendix A

NUMERICAL FILTERING

Appendix A
NUMERICAL FILTERING

The Martin-Graham filter was selected for data smoothing in this investigation primarily because of its efficiency and simplicity. It is efficient in the sense that it requires fewer weights to meet certain response criteria (such as sharp cutoff or strong suppression of high frequencies) than most commonly used filters. On the following pages a listing (in Fortran IV) is provided of a generalized computer subroutine which computes the weights for several filter types, all of which are derived from the basic Martin-Graham low-pass filter. The subroutine may also be called to smooth sets of data. The listing is preceded by a program description which outlines briefly the method by which smoothing weights are derived, and which explains how the subroutine is used.

In general, the response of an ideal low-pass filter is equal to unity up to some cutoff frequency, and equal to zero at all higher frequencies. In practice, such a perfect response is impossible to attain. Usually, as the number of smoothing weights is increased, the filter response becomes more nearly ideal. Computation time becomes greater, however, as does the number of data points which are lost. (If there are 2N+1 weights, the first and last N data points are lost.) As the width of the rolloff interval (f_t-f_c) is decreased, the flatness of the response outside this interval also decreases. Thus, this interval cannot be made too small when strong suppression of the higher frequencies (associated with noise) is required.

The filter selected to smooth Jimsphere ascent-rate data in this investigation has 41 weights, and cutoff and termination frequencies (f_c and f_t) of 0.002 and 0.003 cycles/m, respectively. The response of this filter

is shown in Figure A-1. Because the high-frequency noise in the data is so intense, strong suppression of the higher frequencies was necessary. It was found that a filter having fewer than 41 weights was not capable of the necessary noise suppression while maintaining a fairly narrow rolloff interval. Figure A-1 shows that wavelengths less than 200 m (f = 0.005) are reduced to less than 4% of their original amplitude, and those of less than 100 m (f = 0.01) are reduced to less than 2%. Thus, this filter effectively suppresses these shorter wavelengths.

GFILTR: Numerical Smoothing Routine

Written By: D. Carlin, R. E. De Mandel and S. J. Krivo, Lockheed Missiles & Space Company, Huntsville Research & Engineering Center.

Purpose: To compute the numerical smoothing weights for a low-pass, high-pass, band-pass, or notch filter. Separate entry points, FLDATA and FRRESP, allow the user to apply the filter to any number of sets of data and to compute the filter response.

Method: The basic design is a low-pass Martin-Graham filter (Reference). The gain function, G(f), is defined as:

$$G(f) = 1 \qquad \text{when } f \leq f_c$$

$$G(f) = 1/2 \left[\cos \left(\frac{f - f_c}{f_t - f_c} \pi \right) + 1 \right] \qquad f_c \leq f \leq f_t$$

$$G(f) = 0 \qquad f \geq f_t$$

where:

f_c (the cutoff frequency) = the highest frequency whose amplitude is passed with unity gain.

f_t (termination frequency) = the lowest frequency whose amplitude is passed with zero gain.

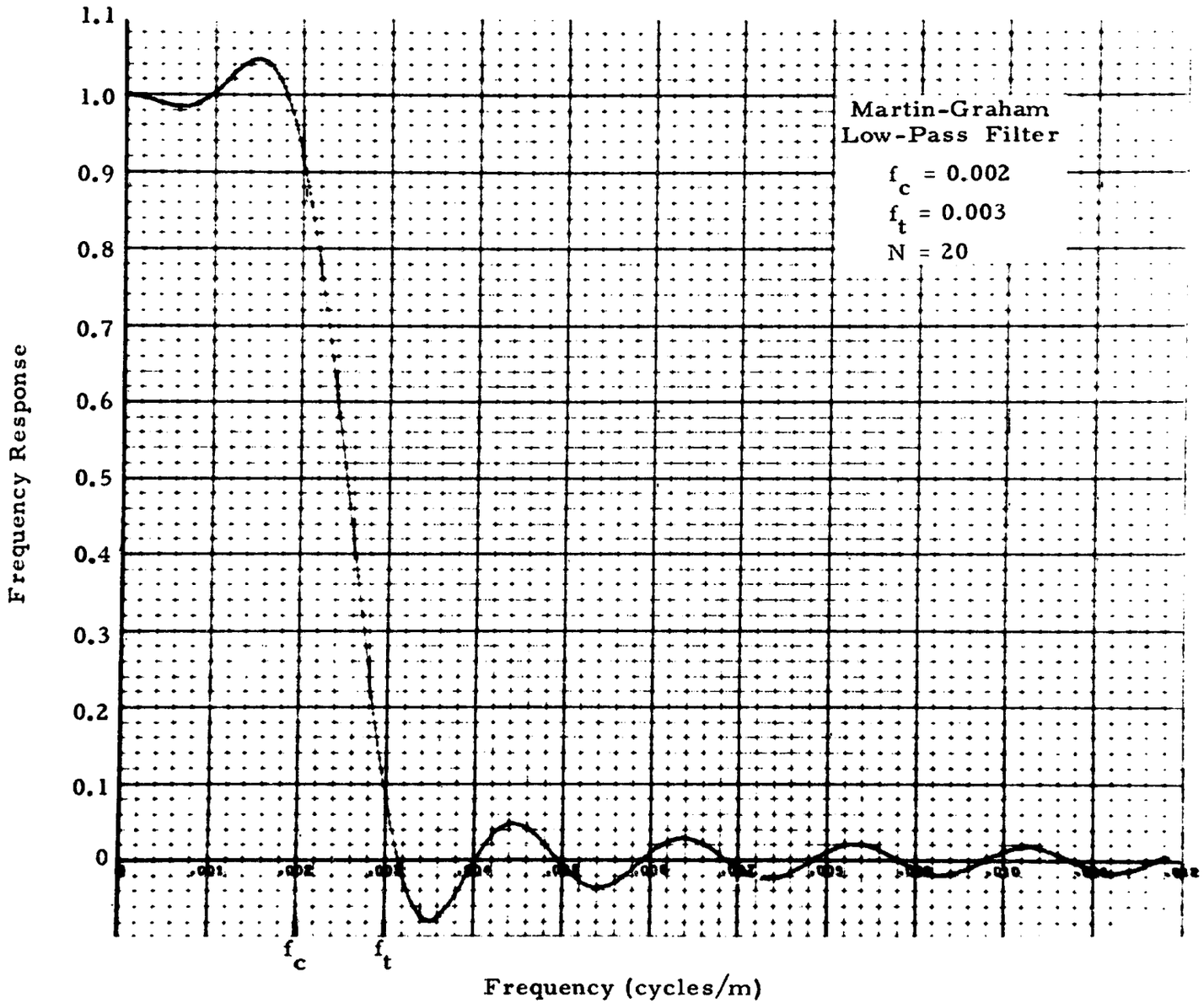

Figure A-1 - Response of the Filter Used to Smooth Jimsphere Ascent-Rate Profiles

Thus the gain function has unity gain below f_c, a cosine function in the rolloff interval between f_c and f_t, and zero gain above f_t. The gain function of this low-pass filter is illustrated in Figure A-2a. (Here, F1 and F2 represent f_c and f_t, respectively.)

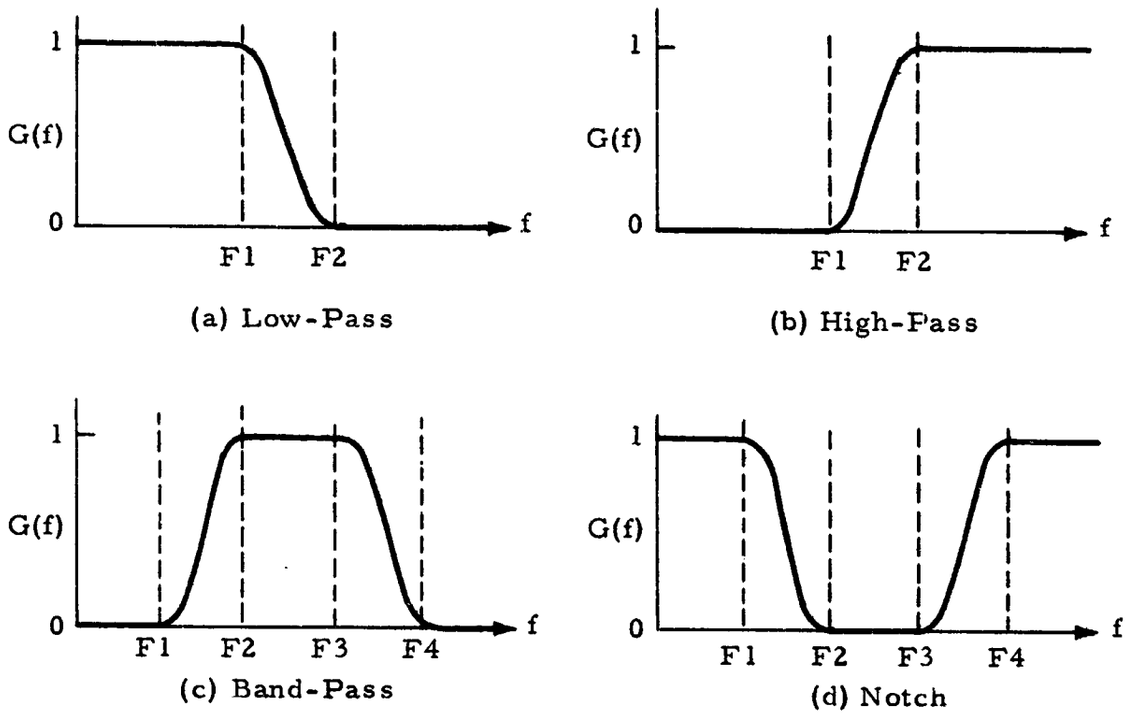

Figure A-2 — The Four Filter Types Which Can Be Generated With GFILTR

The above gain function can be converted, by an inverse Fourier transformation, to the weight function, h(t), in the time (t) domain:

$$h(t) = \frac{\sin(2\pi f_t t) + \sin(2\pi f_c t)}{2\pi t\left[1 - 4t^2 (f_t - f_c)^2\right]} \quad .$$

The discrete sample form of this weight function equation is

$$h_n = h(nT) = \frac{\sin(2\pi f_t nT) + \sin(2\pi f_c nT)}{2\pi nT\left[1 - 4n^2 T^2 (f_t - f_c)^2\right]}$$

where:

T = time interval between data samples

n = weight index (-N, -N+1, . . . , -1, 0, 1, . . . , N-1, N)

N = (NW-1)/2

NW = number of weights

The center weight (n = 0) is given by:

$$h_o = f_c + f_t \quad .$$

When the weights, h_n, have been determined, they are normalized by applying the constraint

$$\sum_{n=-N}^{N} h_n = 1 \quad .$$

Only (N + 1) weights need be calculated since $h_n = h_{-n}$. Since the filter function is even, no phase shift is produced.

The application of the filter to input data (X_J) to produce filtered data (Y_K) is given by:

$$Y_K = h_o X_{N+K} + \sum_{n=1}^{N} h_n (X_{N+K-n} + X_{N+K+n})$$

where K = 1, 2, . . . , NX - 2N, and NX = the number of input (data) points.

The filter response function is given by

$$\hat{G(f)} = h_o + 2 \sum_{n=1}^{N} h_n \cos(2\pi f n T)$$

As the number of weights (NW) is increased, the response of the filter improves [i.e., $\hat{G(f)}$ approaches G(f)]. However, computation time increases as does the number of points lost (the first and last N data points).

The basic low-pass filter is used to design the other filter types (see Figure A-2):

1. The weights for a high-pass filter are obtained by subtracting the weights of a low-pass filter from those of an all-pass filter (one in which all frequencies have unity gain). The weights of an all-pass filter are equal to zero except for the middle weight which is unity.
2. The weights of a band-pass filter are obtained by subtracting the corresponding weights of two low-pass filters.
3. Notch filter weights are obtained by subtracting the band-pass weights from the all-pass weights.

USAGE: The CALL statement for determination of the weights is:

CALL GFILTR (ITF, DELT, NP, W, F1, F2, F3, F4)

where:

ITF specifies the filter type to be generated. ITF may be assigned values from 1 to 4 as follows:

$$ITF = \begin{cases} 1 & \text{low-pass} \\ 2 & \text{high-pass} \\ 3 & \text{band-pass} \\ 4 & \text{notch} \end{cases}$$

DELT is the time interval between successive data points.

NP is the number of weights desired. NP must always be odd.

W is the weight array. W must be dimensioned by at least NP in the main program.

F1, F2, F3, F4 are the desired cutoff and termination frequencies, f_c and f_t. For a low-pass or high-pass filter, values are assigned to F1 and F2, and F3 and F4 are "dummy" arguments. For a band-pass or notch filter two values of f_c and f_t are required. After values are selected for the cutoff and termination frequencies, they must be assigned to F1, F2, F3, and F4 such that $F1 \leq F2 \leq F3 \leq F4$ (see Figure 1).

The CALL statement used to apply the filter to a set of data is:

```
CALL FLDATA (NX, X, Y)
```

where:

NX is the number of data (input) points to be smoothed.

X is the input array of data points. X must be dimensioned by at least NX in the main program.

Y is the output array of filtered data. It must be dimenby at least NX-2N in the main program.

The CALL statement for the filter response is

```
CALL FRRESP (NF, FI, FS, F, R)
```

where:

NF is the number of points (frequencies) for which response is to be computed.

FI is the frequency interval between points.

FS is the first (lowest) frequency at which response is to be computed.

F is the output array of frequencies for which response is computed. F must be dimensioned by at least NF in the main program.

R is the output array of response values. R must be dimensioned by at least NF in the main program.

RESTRICTION: The only restriction on the number of weights (NP) chosen is the amount of core storage available.

REFERENCE: Graham, Ronald J., "Determination and Analysis of Numerical Smoothing Weights," NASA TR R-179, George C. Marshall Space Flight Center, Huntsville, Alabama, December 1963.

SUBROUTINE LISTING
(FORTRAN IV)

```
      SUBROUTINE GFILTR (ITF,DELT,NP,X,F1,F2,F3,F4)
      DIMENSION  W(NP)
      DATA  PI/3.14159265/
           NP1 = (NP + 1) / 2
           I1 = NP1 - 1
           DT2 = 2.0 * DELT
           PI2DT = PI * DT2
           KM = 0
           FC = F1
           FT = F2
    1      FTMC = FT - FC
           WX = FT + FC
           SUM = WX
      DO 20 M=1,I1
           K = M + KM
           AA = DT2 * FLOAT(K)
           AM = AA * PI
           AC = AM * FC
           AT = AM * FT
           AL = (FTMC * AA)**2
           AA = 1.0 - AL
        IF (ABS(AL).GE.0.0001) GO TO 15
           X(M) = (SIN(AT) - SIN(AC)) / (AM + AM)
        GO TO 20
   15      X(M) = (FT*COS(AT) + FC*COS(AC)) / (1.0 - 0.5*AL)
   20 SUM = SUM + 2.0*W(M)
           K1 = KM + 1
           K2 = KM + 2
      DO 30 M=K1,K2
   30 X(M) = W(M) / SUM1
           XX = XX / SUM1
      IF (ITF.EQ.1) GO TO 40
           X(NP1) = XX
      IF (ITF.LT.2) GO TO 50
      IF (ITF.EQ.2) GO TO 3
           FC = F3
           FT = F4
```

```
      KM = NP1
      GO TO 10
25    DO 27 K=1,N
      M = K + NP1
27    X(K) = X(K) - X(M)
      X(NP1) = DX - X(NP1)
      IF (ITF.EQ.3) GO TO 29
      X(NP1) = 1.  - X(NP1)
      DO 30 I=1,N
30    W(K) = -W(K)
      GO TO 99
      ENTRY FLOATA (NX,X,Y)
      DIMENSION X(NX),Y(NX)
      KM = NX - N - 1
      DO 42 K = 1,KM
      M = K + N
      SUM = X(M)*W(NP1)
      DO 40 J=1,N
      M1 = M - J
      M2 = M + J
40    SUM = SUM + W(J)*(X(M1) + X(M2))
42    Y(K) = SUM
      GO TO 99
      ENTRY FIRFLT (NF,FI,F,E,D)
      DIMENSION F(NF),E(NF)
      F(1) = FI
      DO 50 K=2,NF
50    F(K) = F(K-1) + FI
      DO 60 I=1,NF
      E(I) = X(NP1)
      DX = F(I) * PI/D
      DO 60 J=1,N
60    E(I) = E(I) + 2.0 * W(J) * COS(FLOAT(J) * DX)
99    RETURN
      END
```

Appendix B

DERIVATION OF THE EQUATION OF MOTION OF A JIMSPHERE WIND SENSOR RISING THROUGH A MOTIONLESS ATMOSPHERE

Appendix B

DERIVATION OF THE EQUATION OF MOTION OF A JIMSPHERE WIND SENSOR RISING THROUGH A MOTIONLESS ATMOSPHERE

Consider a constant-volume balloon rising through a quiescent atmosphere. The three forces acting on the balloon are: (1) the weight of the balloon and its gas, (2) buoyancy, and (3) drag. The total weignt, W, of the balloon and gas is given by:

$$W = -g(m + m_H) \tag{B.1}$$

where m is the mass of the uninflated balloon, and m_H is the mass of the enclosed helium. The buoyancy force, B, is equal to the weight of air displaced by the balloon:

$$B = \rho V g \tag{B.2}$$

where ρ is the density of air, V is the volume of the balloon, and g is the acceleration due to gravity. The drag force, D, acting on the balloon is given by:

$$D = \frac{-C_D}{2} \rho w^2 A \tag{B.3}$$

where C_D is the drag coefficient, w is the ascent rate of the balloon, and A is the cross-sectional area of the balloon.

In free ascent, the balloon soon reaches a state of equilibrium where the three forces come into balance. Thus, the balloon's acceleration vanishes, i.e.,

$$B + D + W = 0 \tag{B.4}$$

Substituting Equations (B.1), (B.2) and (B.3) into (B.4), we obtain

$$\rho V g = \frac{C_D}{2} \rho w^2 A + g(m + m_H) \tag{B.5}$$

The equation of state for helium is

$$m_H = \frac{p_b V}{R_H T_b} \tag{B.6}$$

where p_b and T_b are the pressure and temperature of the helium, and R_H is the gas constant for helium. The Jimsphere is equipped with valves which maintain a constant internal superpressure, s, of 5 mb. Therefore,

$$p_b = p + s \tag{B.7}$$

where p is the environmental air pressure. The internal temperature, T_b, of the balloon may be expressed as the sum of the outside ambient temperature T and some deviation δT:

$$T_b = T + \delta T . \tag{B.8}$$

The constant, R_H, may be expressed as

$$R_H = k R \tag{B.9}$$

where R is the gas constant for dry air and k is the ratio of the molecular weight of air to the molecular weight of helium.

From Equations (B.6), (B.7), (B.8), (B.9) and the ideal gas law, we obtain

$$m_H = \frac{(p+s)\,V}{R_H\,T_b} = \frac{\rho\,R\,T V}{R_H\,T_b} + \frac{sV}{R_H\,T_b} = \frac{\rho V(T_b - \delta T)}{k\,T_b} + \frac{sV}{kR\,T_b}$$

$$= \frac{\rho V}{k}\left(1 - \frac{\delta T}{T_b}\right) + \frac{sV}{kR\,T_b} \quad . \tag{B.10}$$

Combining Equations (B.5) and (B.10) and rearranging terms yields

$$C_D\,w^2 = \frac{2g}{\rho A}\left[\rho V - \left(m + \frac{\rho V}{k} - \frac{\rho V\,\delta T}{k\,T_b} + \frac{sV}{kR\,T_b}\right)\right]$$

$$= \frac{2g\,V}{A}\left(1 - \frac{1}{k}\right) - \frac{1}{\rho}\left(\frac{2gm}{A} + \frac{2gsV}{A\,kR\,T_b}\right) + \frac{2gV\,\delta T}{kA\,T_b} \quad .$$

This equation is of the form

$$C_D\,w^2 = C_1 - \rho^{-1}\left(C_2 + \frac{C_3}{T_b}\right) + C_4\,\frac{\delta T}{T_b} \quad . \tag{B.11}$$

The four constants C_i are evaluated, assuming

Jimsphere radius = 1 m
m = 407.9 g
s = 5 mb .

Making these substitutions, we obtain (in c.g.s. units)

$$C_1 = \frac{2g\,V}{A}\left(1 - \frac{1}{k}\right) = 2.26 \times 10^5$$

$$C_2 = \frac{2g\,m}{A} = 25.5$$

$$C_3 = \frac{2g\ sV}{AkR} = 63.1$$

$$C_4 = \frac{2g\ V}{kA} = 3.61 \times 10^4 .$$

Equation (B.11) thus becomes

$$C_D\, w^2 = 2.26 \times 10^5 - \frac{1}{\rho}\left(25.5 + \frac{63.1}{T_b}\right) + 3.61 \times 10^4\ \frac{\delta T}{T_b} . \qquad (B.12)$$

This result may be further simplified by noting that during a Jimsphere flight, T generally varies between 200°K and 300°K, ρ varies from about 1.2×10^{-3} g/cm^3 to 1.3×10^{-4} g/cm^3, and $|\delta T|$ is probably no larger than 10°C. Considering these magnitudes it can be seen that the two terms in Equation (B.12) containing T_b are about two orders of magnitude smaller than the others. Thus, they can be neglected with only a small loss of accuracy. We thereby obtain a simple expression for w as a function of ρ and C_D:

$$w \cong \left[\frac{1}{C_D}\left(2.26 \times 10^5 - 25.5\ \rho^{-1}\right)\right]^{1/2} . \qquad (B.13)$$